Australian Earthquake Engineering Society
2022 National Conference, 24-25 November 2022
Mount Macedon, Victoria, Australia

Making URM buildings safer in provincial towns - Cost-effective earthquake solutions

Marta Giaretton[1], Jason Ingham[2] and Dmytro Dizhur[1]

1. Dizhur Consulting, Auckland, New Zealand
2. Department of Civil & Environmental Engineering, University of Auckland, New Zealand

Abstract

Following the 14 November 2016 the Mw 7.8 Kaikoura, New Zealand earthquake, the Ministry for Business, Innovation and Employment together with representatives from local government, researchers and practitioners discussed possible strategies for how to address the elevated risk of fatalities posed by unreinforced masonry (URM) façades and parapets. The outcome was a policy (successfully implemented) that required securing of street-facing parapets and façade with a particular focus on heritage precincts with high pedestrian traffic.
In parallel, an experimental campaign was undertaken to provide building owners and practicing engineers with a better understanding of the performance of different levels of building strengthening and also propose simple, speedy and cost-effective retrofit solutions.
The experimental campaign involved testing on a shaking table scaled replicas of traditional two-storey unreinforced clay brick masonry commercial buildings. The building performance was first tested in the as-built condition in order to establish a benchmark for the proposed retrofit techniques. Two different levels of strengthening were investigated: (i) simple wall-to-diaphragm connections, (ii) additional vertical strong-backs installed on the top floor wall interior surface and moment-resisting frames placed at the ground floor. Scaled building and material characteristics as well as the obtained results during the shaking table tests in terms of response of the structure, damage mechanisms and performance achieved are reported herein.

Keywords: URM Seismic retrofit, Strong-backs, Mechanical Anchors, Shake table testing

1 Introduction

The poor performance of unreinforced masonry (URM) buildings in past earthquakes throughout the world in locations such as New Zealand [1, 2], Italy [3, 4], California [5], and Nepal [6] is well documented. Post-earthquake observations highlighted also cases where the seismic retrofits did not consistently perform in accordance with their design [7, 8]. Hence it is important to investigate and test simple, reliable, and cost-effective retrofit techniques that are suitable for specific building typologies. In addition, a recent Building Amendment Act [9] in New Zealand requires all earthquake vulnerable buildings to be either strengthened or demolished within the next 15-25 years, and hence providing engineers and contractors with proof-tested cost-effective techniques will allow to building owner to best comply the Government exportations. In response to this need, shake-table testing of a commonly encountered New Zealand and Australia URM building was undertaken considering minimal

retrofit and retrofitted scenarios. The aim of the experimental campaign was to enhance understanding of the sequence of damage that leads to the formation of different collapse mechanisms and to closely investigate the effectiveness of various retrofit interventions.

Two quarter-scaled clay-brick URM building models were constructed as representative of the common vintage commercial two-storey row buildings with multiple occupancies in New Zealand (URM building typology D, [17]) and Australia, see **Figure 1a**. The building consisted of a symmetrical opening configuration on the front façade with a large shop window at the ground floor and two smaller windows at the first floor see **Figure 1b**), and an asymmetrical opening configuration at the back façade with a door at the ground floor and two windows at the first floor. One of the side walls had two asymmetrical windows at the top floor (see **Figure 1b**) suggesting that the model was representative of an end-row building. General building and model dimensions are presented in **Table 1**. The first building model was tested in as-built conditions with wall-to-diaphragm (w-to-d) anchorages while the second building model was tested in retrofitted condition. The retrofits were designed to be cost-effective and to be easily implement and removed if needed. Reversibility of the retrofit interventions is desirable for existing buildings as it enables eventual removal of the retrofits for more aesthetic or advanced replacement solutions without damaging the original masonry fabric.

(a) Typical row buildings in Australia

(b) View of the model front facade and right side

***Figure 1**: Example of typical building typology and replicated building model*

2 Models construction

400 clay-bricks were sourced from the demolition of an existing 1930's vintage villa and cut to half scale, resulting in an average dimensions of 110L x 50W x 40T (mm). The half scaled bricks were laid in a running bond pattern and proportionally replicated the thickness of a two-brick thick wall without over complicate the model construction. It is recognized that using ½ scale bricks halved the number of courses in the model, possibly increasing stiffness and strength of the model when comparing to the case of ¼ scaled bricks [18]. The mortar mix used was a 1:3 lime:sand in order to represent the typical low compressive strength of existing weathered and deteriorated ultra-weak mortar often encountered in the New Zealand and Australia existing building stock [19]. Materials compressive strength identified via laboratory testing in accordance with [20–22] are presented in **Table 2**.

***Table 1:** Building model dimensions*

Dimension	Typical building typology	Model
Length	8.00m	2.00m
Width	4.00m	1.00m
Height (front)	8.00m	1.65m
Height (side)	7.00m	1.50m
Wall thickness	0.22m	0.05m

***Table 2**: Material properties*

Material	Average Compressive Strength (MPa)	
	As-built model	Retrofitted model
Bricks	17.8 MPa	17.8 MPa
Mortar	0.23 MPa	0.22 MPa
Masonry Prisms	-	4.62 MPa

The walls were fixed at the base by screwing thin timber sections on both sides of the wall to avoid sliding during testing. Timber lintels were replicated above openings. The floor and roof diaphragms were constructed using 6 mm thick medium-density fibreboard (MDF) screwed @30 mm c/c spacing to the perimeter beams.

2.1 As-built model with w-to-d anchorages

To ensure a box-type behavior and avoid cantilever wall collapse, a minimal level of retrofit was installed in the as-built model and consisted of wall-to-diaphragm connections at both floor and roof level as founded in many existing buildings. The connections were realised by bolting the timber floor section to the wall through the mortar joints, see **Figure 2a**.

2.2 Retrofitted model

In addition to the wall-to-diaphragm connections (see **Figure 2a**), two moment-resisting frames (MRF) were placed on the ground floor of the retrofitted model, as shown in **Figure 2b**, to resist the majority of the flexural demand. The MRF were composed of equally spaced 75 mm x 50 mm timber sections, and were screwed into the MDF floor board above and also the shake-table base below. Lateral load would transfer from the wall, through the floor, into the frames, and then finally into the shake-table base.

(a) Wall-to-diaphraghm connections

(b) Moment resisting frames

(c) Timber strong-backs and shear wall layout at the first floor

***Figure 2**: Retrofitted building model scheme*

On the top floor, 18 mm x 25 mm timber strong-backs replicating the cost-effective technique proposed in [23] were installed as shown in **Figure 2c**. The top and bottom sections of the timber strong backs were screwed into the roof and floor respectively, to enable load path transfer from the diaphragms to the walls. Each vertical strong-back member was then bolted into the wall to create a composite action reducing the risk of out-of-plane collapses in the top storey. Shear walls composed of 6 mm MDF board were introduced on the in-plane walls and bolted to the piers, see **Figure 2c**, to reduce the rocking demand of the piers at the first floor characterised by high aspect ratio and low axial load.

3 Testing procedure and instrumentation

Eleven wired accelerometers (red marked) and twenty wireless accelerometers (yellow marked) were installed around the buildings to measure accelerations, see **Figure 3**. Three displacement devices, marked in white in **Figure 3**, were used to measure the table, floor and roof displacements.

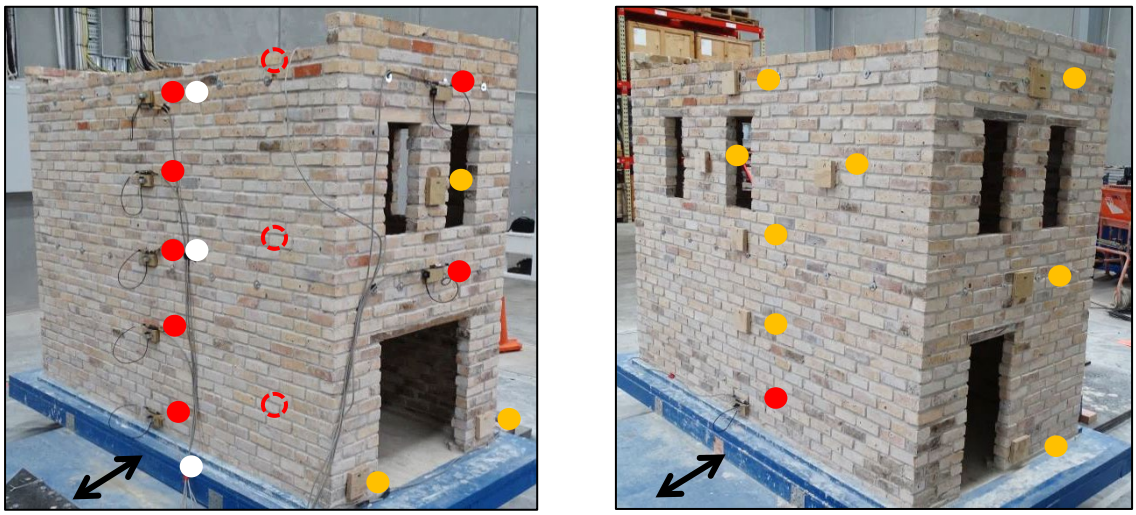

(a) Front façade and left-side wall (b) Back façade and right-side wall

Figure 3: *Instrumentation layout where red and orange marks are wired and wireless accelerometers respectively, and white marks are displacement devices*

Eight cameras were placed in strategic locations around the building model to record the visual shaking behaviour of the structure for detailed analysis after completion of testing. Two 360° cameras were installed at the centre of the ground and first floor to monitor the dynamic behaviour and damages on the inside of the building model.

A monotonic sinusoidal time-history was applied in the direction of the black arrow shown in **Figure 3**. A sweep test was then undertaken, gradually increasing the frequency (and thus acceleration) of the shake-table motor until the model reached a predetermined level of damage. Three tests were completed, each reaching greater maximum accelerations and higher level of damage pattern (low damage, medium damage and collapse). The instrumentation was then removed prior the final test which led to collapse. The as-built model underwent over 400 cycles of shaking, while the retrofitted model was tested for 27 minutes in total with exactly 1001 cycles.

4 Results: As-built model with w-to-d anchorages

4.1 Crack-pattern

Figure 4 shows the crack-pattern observed on each wall of the as-built model during all stages of testing. Pink lines represent existing cracks prior testing, blue lines represent low damage step and black lines refer to medium damage test.

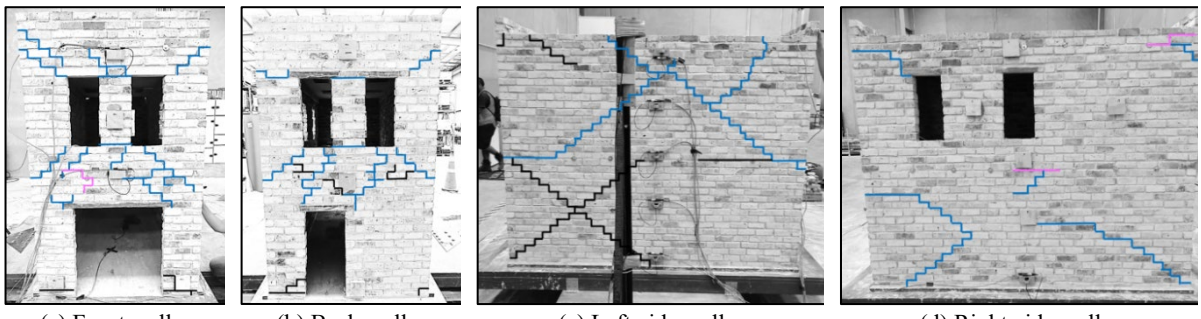

(a) Front wall (in-plane) (b) Back wall (in-plane) (c) Left-side wall (out-of-plane) (d) Right-side wall (out-of-plane)

Figure 4: *Crack-patterns observed following each test in the as-built model*

Figure 4a,b show in-plane damage with prominent cracks extending from all openings in the front and back building facades. Most of these cracks initiated at low accelerations and

widened throughout testing. The main damage on the in-plane walls was concentrated on the spandrels above the floor connection. Rocking of the ground floor in-plane piers occurred at high accelerations, and so the cracks at the bottom of these faces were only observed in the medium damage test. Referring to the face-loaded walls, textbook-type two-way bending failure was observed as the dominant crack-pattern in the left-side wall as shown in **Figure 4c**. This initiated at the second storey, which eventually caused top floor building collapse, and then in the bottom storey occurred at higher accelerations. However, despite the presence of two windows, cracking was only minor in the right-side wall displayed in **Figure 4d**.

4.2 Damage progression

Low damage – Many diagonal cracks propagated from the corners of the in-plane openings at low accelerations with the first in-plane cracking being clearly visible at approximately 0.3g. Cracks in the out-of-plane walls appeared at approximately 0.43g leading to a maximum displacement at the roof level of approximately 18 mm. Initiation of rocking of ground floor in-plane piers was observed with the top storey showing a slight swaying motion.

Medium damage – At an acceleration of approximately 0.36g the existing in-plane cracks widened substantially up to building instability. The second storey began rocking about these cracks which induced out-of-plane movements on the face-loaded walls. Clear two-way bending was observed in the top-storey of the left-side wall (see **Figure 5b**) and also initiated at the ground floor of the right-side wall inducing the entire building to start slight rocking. Cracks formed at the end of the central window piers in the front and back facades but the pier didn't collapse.

Collapse – As the acceleration increased, two-way bending crack-patterns appeared at the lower storey of the left-side wall, see **Figure 5b**. As the acceleration reached approximately 0.56g, two large cracks extending from the upper and lower corners of the front-right window caused the whole section of the right-side wall to separate from the structure, see **Figure 5a**. The upper-storey showed a clear two-way bending followed by full collapse, while the lower storey was standing and showing extensive cracks.

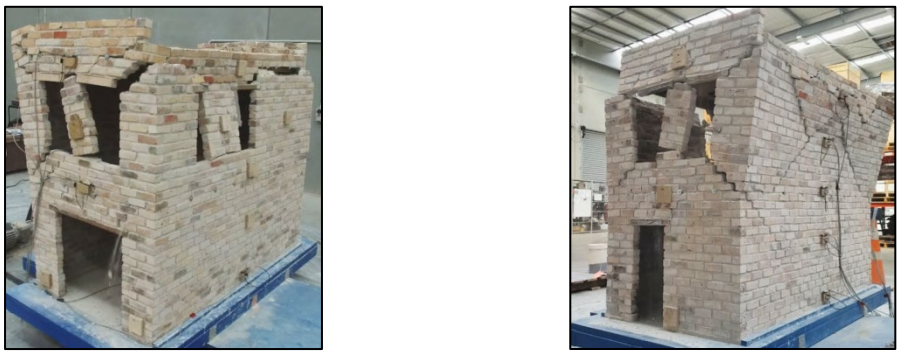

(a) Front façade and right-side wall (b) Back façade and left-side wall

Figure 5: *As-built building model at near-collapse, 0.56g*

5 Results: Retrofitted model

5.1 Crack-pattern

Figure 6 shows the crack-patterns experienced by each wall during all stages of testing. Pink lines represent existing cracks prior testing, blue lines represent low damage step and black lines refer to medium damage test. The solid regions show areas of collapse and are colored to indicate the test the collapse occurred in. **Figure 6a,b** show the prominent cracks extending from all openings in the in-plane (front and back) building facades, some of which were pre-existing and extended in width and length during subsequent testing. A large diagonal crack spread diagonally across the back façade, and its progression is shown by the red arrows in **Figure 6b**. This cracking coincided with the onset of two-way bending on the ground floor of the left-side wall, and eventually caused a local collapse during the low damage test.

The dominant crack-pattern on the left-side wall was the textbook-type two-way bending shown in **Figure 6c**. This was dominant in the bottom storey, while less strong on the top storey. However, for both storeys the cracking was only minor in the right-side wall displayed in **Figure 6d**, despite the presence of two windows.

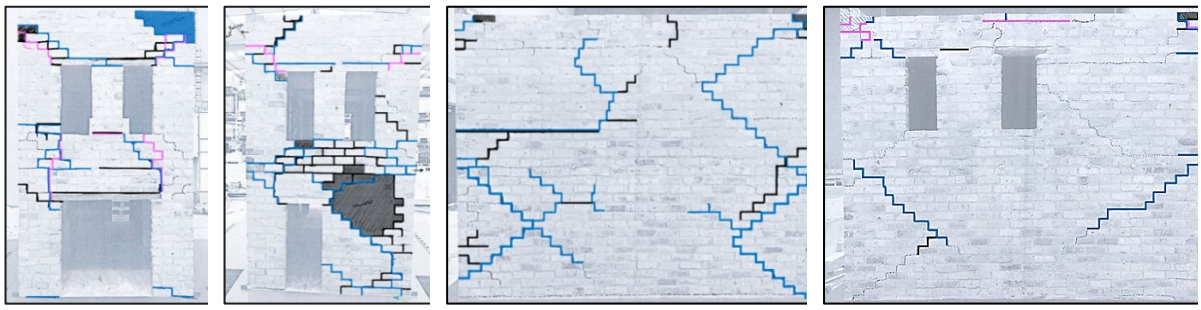

(a) Front façade (in-plane) (b) Back façade (in-plane) (c) Left-side wall (out-of-plane) (d) Right-side wall (out-of-plane)

Figure 6: *Crack-patterns observed following each test in the retrofitted building model*

5.2 Damage progression

Low damage – Initiation of rocking of ground floor in-plane piers was observed at an acceleration of approximately 0.35g. This was especially prominent in the front facade, on which there was also noticeable rocking of the pier between the windows. Diagonal cracks propagated from the corners of the openings, causing damage in the corner of the back facade and left-side wall. There was a combination of shear cracking extending from the back door, as well two-way bending on the first storey of the left-side wall which commenced at an acceleration of about 0.65g inducing top floor to start swaying. A corner of the front parapet collapsed at approximately 0.70g. The maximum displacement recorded at mid-span of the left-side wall was approximately 26 mm and 21 mm at roof level and floor level respectively.

Medium damage – Upon re-testing, the building behaved very similarly to the previous low damage test. At approximately 0.5g cracking initiated in the back parapet. As the acceleration increased above 0.6g new cracks formed in the front and back spandrels. The mortar joints in the front window pier split, and stability was fully provided by the shear wall. A local collapse occurred in the front parapet at approximately 0.85g. The diagonal cracking in the ground floor pier on the back facade formed a local collapse at an acceleration of 0.9g. Two-way bending commenced in the upper storey of the left-side wall but still wasn't present in the right-side wall. The maximum displacement recorded at mid-span of the left-side wall was approximately 44 mm and 23 mm at roof level and floor level respectively.

Collapse – As the accelerations increased, widening cracks caused several local collapses. Global collapse eventually occurred due to two-way bending in the right-side wall, and the retrofit structure remained intact.

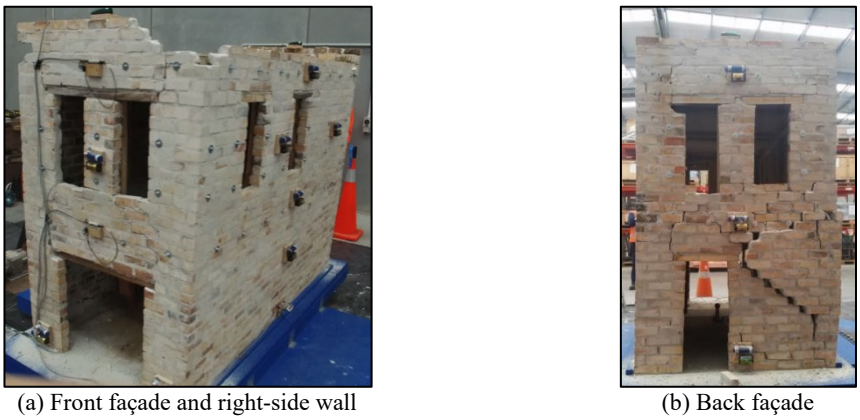

(a) Front façade and right-side wall (b) Back façade

Figure 7: *Retrofitted building model at near-collapse, 0.90g*

6 Data analysis

Figure 8a,b shows acceleration profiles along the building height, normalised with respect to the peak ground acceleration (PGA) measured on the table. Data is shown at several locations, for both the as-built and retrofitted models. **Figure 8c** compares the PGA recorded at different level of damage above described and shows in brackets the percentage of acceleration increment between as built and retrofitted models. The maximum recorded roof displacement measured at mid-span of the left-side wall was 56 mm and 44 mm for as-built and retrofitted models respectively. After completion of testing, the retrofitted model presented a residual 18 mm displacement toward the left-side wall.

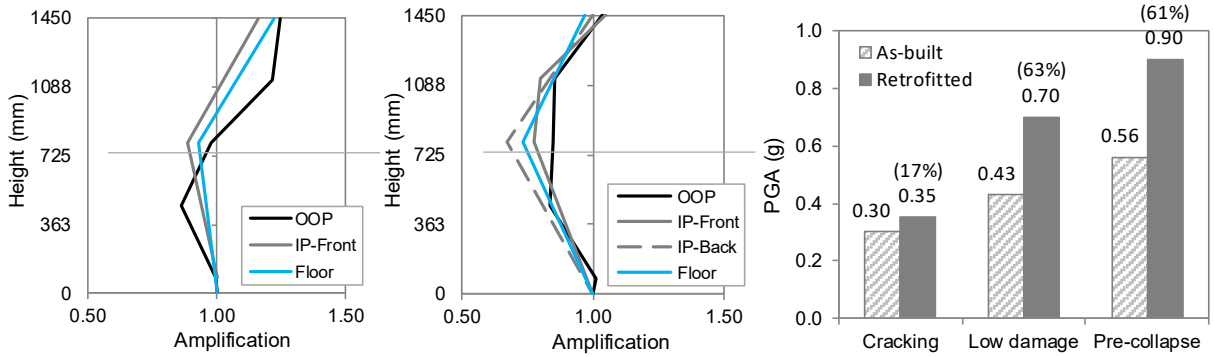

(a) Normalised acceleration up the as-built building, near-collapse

(b) Normalised acceleration up the retrofitted building, near-collapse

(c) PGA at different level of damage (% refers to the increment in PGA comparred to as-built)

Figure 8: *Acceleration comparison between models*

In the retrofitted model it was possible to monitor and capture also a clear torsional response of the structure which is displayed in **Figure 9**. Data in the graph represent the normalised maximum accelerations at three locations on the first floor. At all stages of testing the front face had significantly higher accelerations than the rest of the building, which was likely due to the lack of symmetry and large opening.

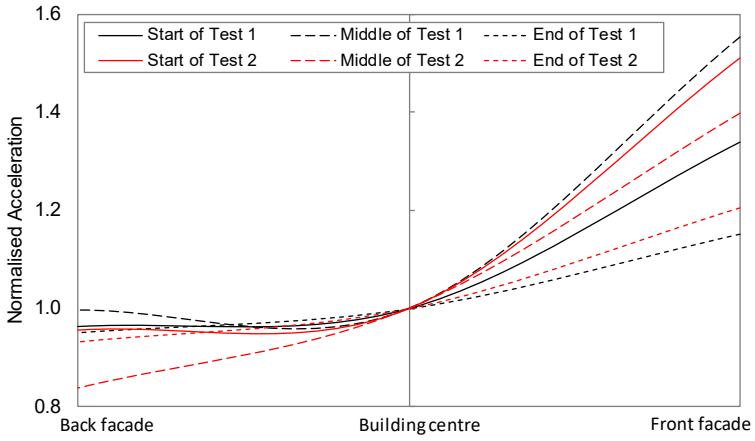

Figure 9: *Normalised acceleration along the first floor*

7 Retrofit performance

The retrofitted model remained stable until collapse occurred despite significant accelerations and in-plane cracking. The integrated timber strong-back and moment frame retrofit tied the building together as a whole structure (aka 'box-type' behaviour), rather than each storey acting independently up to full collapse of the top storey as occurred in the as-built model. The moment-resisting frames took significant flexural demands preventing early collapse of the ground floor. However, significant torsional displacements were observed in particular in the front face compared to the building centre. It is possible that placing the frames closer to the

in-plane facades would have resulted in an overall stiffer structure and lower accelerations at the front wall limiting the development of the crack-pattern.

As observed in the as-built model, the top storey was expected to be the first to undergo two-way out-of-plane bending due to reduced axial load and increased acceleration than the ground floor. However, in the retrofitted model two-way bending initiated in the ground floor at approximately 0.65g, and the first floor of the right-side wall didn't show any signs of two-way bending until total collapse which occurred over 0.90g. This indicated that the timber strong-back retrofit increased the strength of the first floor walls enough to resist substantially higher out-of-plane accelerations than the non-retrofitted ground floor. The strong-backs stiffened the top storey and cracks propagated to the lower floor causing more widespread damage and hence release of energy significantly delaying the collapse. In conclusions, the as-built model collapsed at a shake-table acceleration of 0.56g after 260 cycles of shaking, while the retrofitted model withstood accelerations of up to 0.9g before the accelerometers were removed and survived 1000 cycles demonstrating the vast increase in resilience provided by the retrofits.

8 Conclusions

The experimental campaign consisted in testing two quarter-scaled clay-brick URM building models, one in as-built conditions with wall-to-diaphragm anchorages and the second one in retrofit conditions. The buildings are representative of common vintage commercial two-storey row buildings in New Zealand and Australia. The testing was undertaken using a shake-table and provided the following conclusions:

- The testing realistically reproduced classic failure mechanisms including two-way bending, in-plane diagonal cracking, and rocking at the base of the piers observed during post-earthquake field observations.

- Strong torsional behaviour was exhibited at all stages of testing, as a result of the structural asymmetry (openings).

- Cracking initiated on both models at approximately 0.3/0.35g and rapidly propagated in the as-built building up to full collapse of the top-storey at 0.56g. The retrofitted model showed high resilience and was still standing at 0.9g (61% higher PGA than as-built) despite significant damage widespread through the entire building. The retrofitted model resisted four times the number of cycles sustained by the as-built one.

- On the strengthening techniques tested:

    - The simple bolted wall-to-diaphragm connections prevented catastrophic failure at low accelerations also for the as-built model.

    - The moment-resisting frames prevented the building from toppling despite rocking of ground floor in-plane piers was observed.

    - Shear wall significantly limited the rocking of the top-storey piers restraining them from collapse.

    - The timber strong-backs prevented two-way bending of the top-storey walls.

The strengthening techniques chosen for this testing are only an example of a possible combination of solutions, each building need to be assessed by a competent engineer and the strengthening methodology proposed needs to be tailored to the specific building.

9 Acknowledgments

The authors wish to sincerely thank NZSEE, Quakecore and EQC who provided partial funding for this experimental campaign and BBR Contech for providing testing facilities. The effort done by Caitlin J. Cairncross and Michael R. Kennerley during testing is also acknowledged.

10 References

1. Dizhur D, Ingham J, Moon L, et al (2011) Performance of masonry buildings and churches in the 22 February 2011 Christchurch Earthquake. Bull New Zeal Soc Earthq Eng 44:279–296
2. Moon L, Dizhur D, Senaldi I, et al (2014) The demise of the URM building stock in Christchurch during the 2010-2011 Canterbury earthquake sequence. Earthq Spectra 30:253–276 . doi: 10.1193/022113EQS044M
3. D'Ayala DF, Paganoni S (2011) Assessment and analysis of damage in L'Aquila historic city centre after 6th April 2009. Bull Earthq Eng 9:81–104 . doi: 10.1007/s10518-010-9224-4
4. Penna A, Morandi P, Rota M, et al (2013) Performance of masonry buildings during the Emilia 2012 earthquake. Bull Earthq Eng 12:2255–2273 . doi: 10.1007/s10518-013-9496-6
5. The Masonry Society (1994) Performance of masonry structures in the Northridge, California earthquake of January 17, 1994. A report by the Investigating Disasters Reconnaissance Team. Austin, Texas
6. Dizhur D, Dhakal RP, Bothara J, Ingham J (2016) Building typologies and failure modes observed in the 2015 Gorkha (Nepal) earthquake. Bull New Zeal Soc Earthq Eng 49:211–232
7. Dizhur D, Ismail N, Knox C, et al (2010) Performance of unreinforced and retrofitted masonry buildings during the 2010 Darfield Earthquake. Bull New Zeal Soc Earthq Eng 43:321–339
8. Giaretton M, Dizhur D, da Porto F, Ingham J (2016) Post-earthquake reconnaissance of unreinforced and retrofitted masonry parapets. Earthq Spectra 32:2377–2397 . doi: 10.1193/121715EQS184M
9. MBIE (2016) Building (Earthquake-prone Buildings) Amendment Act. Public Act 2016 No 22, Ministry of Business, Innovation, and Employment, New Zealand
10. Tomazevic M, Velechovsky T (1992) Some aspects of testing small-scale masonry building models on simple earthquake simulators. Earthq Eng Struct Dyn 21:945–963 . doi: 10.1002/eqe.4290211102
11. Bothara JK, Dhakal RP, Mander JB (2010) Seismic performance of an unreinforced masonry building: An experimental investigation. Earthq Eng Struct Dyn 39:45–68 . doi: 10.1002/eqe.932
12. Benedetti D, Carydis P, Pezzoli P (1998) Shaking table tests on 24 simple masonry buildings. Earthq Eng Struct Dyn 27:67–90 . doi: 10.1002/(SICI)1096-9845(199801)27:1<67::AID-EQE719>3.0.CO;2-K
13. Kallioras S, Guerrini G, Tomassetti U, et al (2018) Experimental seismic performance of a full-scale unreinforced clay-masonry building with flexible timber diaphragms. Eng Struct 161:231–249 . doi: 10.1016/j.engstruct.2018.02.016
14. Magenes G, Penna A, Senaldi IE, et al (2014) Shaking table test of a strengthened full-scale stone masonry building with flexible diaphragms. Int J Archit Herit 8:349–375 . doi: 10.1080/15583058.2013.826299
15. Bairrão R, Falcão Silva MJ (2009) Shaking table tests of two different reinforcement techniques using polymeric grids on an asymmetric limestone full-scaled structure. Eng Struct 31:1321–1330 . doi: 10.1016/j.engstruct.2008.04.039
16. Mazzon N, Chavez Cano MM, Valluzzi MR, et al (2010) Shaking table tests on multi-leaf stone masonry structures: analysis of stiffness decay. Adv Mater Res 133:647–652 . doi: 10.4028/www.scientific.net/AMR.133-134.647
17. Russell AP, Ingham JM (2010) Prevalence of New Zealand's unreinforced masonry buildings. Bull New Zeal Soc Earthq Eng 43:182–202
18. Petry S, Beyer K (2014) Scaling unreinforced masonry for reduced-scale seismic testing. Bull

Earthq Eng 12:2557–2581

19. Lumantarna R, Biggs DT, Ingham JM (2014) Compressive, flexural bond, and shear bond strengths of in situ New Zealand unreinforced clay brick masonry constructed using lime mortar between the 1880s and 1940s. J Mater Civ Eng 26:559–566 . doi: doi:10.1061/(ASCE)MT.1943-5533.0000685
20. ASTM C109 (2013) Standard test method for compressive strength of hydraulic cement mortars. American Society for Testing and Materials, USA
21. ASTM C67 (2017) Standard test methods for sampling and testing brick and structural clay tile. American Society for Testing and Materials, USA
22. ASTM C1314 (2016) Standard test method for compressive strength of masonry prisms. American Society for Testing and Materials, USA
23. Dizhur D, Giaretton M, Giongo I, Ingham J (2017) Seismic retrofit of masonry walls using timber strong-backs. Struct Eng Soc J - SESOC 30:30–44